Palli et al. 2017. *Int. J. Vehicle Structures & Systems*, 9(1), 57-63
ISSN: 0975-3060 (Print), 0975-3540 (Online)
doi: 10.4273/ijvss.9.1.12

International Journal of Vehicle Structures & Systems
Available online at www.maftree.org/eja

Dynamic Behaviour of a 7 DoF Passenger Car Model

Srihari Palli[a,b], Rakesh Chandmal Sharma[c,d] and P.P. Dhanunjaya Rao[a,e]

[a]*Mech. Engg. Dept., Aditya Inst. of Tech. and Management, Tekkali, Andhra Pradesh, India*
[b]*Email: srihari.palli@gmail.com*
[c]*Mech. Engg. Dept., Maharishi Markandeshwar University, Mullana, India*
[d]*Email: drrcsharma@mmumullana.org*
[e]*Corresponding Author, Email: ppdhanu1990@gmail.com*

ABSTRACT:

Conventional vehicle suspension systems, which are passive in nature consists of springs with constant stiffness and dampers with constant damping coefficient. These suspension systems cannot meet the characteristics such as ride comfort, road handing and suspension deflection during abnormal road conditions simultaneously. Active and semi-active suspension systems are the solutions to achieve the desired suspension characteristics. Since, active system is bulky and requires high energy for working, a semi-active suspension system is considered in the present work to analyze vehicle traversing over various road profiles for ride comfort. Mathematical model of a 7 DoF passenger car is formulated using Newton's method. A semi-active suspension system with skyhook linear control strategy avoids the road excitations at resonant frequencies by shifting the natural frequencies of the model by varying damping coefficients based on the vehicle response for different road conditions where the excitations could be harmonic, transient and random. Modal analysis is carried out to identify the un-damped natural frequencies and mode shapes for different values of damping. The above analyses are carried out through analytical and numerical methods using MATLAB and ANSYS software respectively and the results obtained from both are in good agreement.

KEYWORDS:

Dynamic response; Modal analysis; Natural frequency; Mathematical model; ANSYS; MATLAB

CITATION:

S. Palli, R.C. Sharma and P.P.D. Rao. 2017. Dynamic Behaviour of a 7 DoF Passenger Car Model, *Int. J. Vehicle Structures & Systems*, 9(1), 57-63. doi:10.4273/ijvss.9.1.12.

ACRONYMS AND NOMENCLATURE:

M, M_i	Sprung and Unsprung mass
K_{Ui}, C_{Ui}	Tire stiffness and damping coeff.
K_{Si}	Suspension stiff. between sprung & unsprung mass
C_{Si}	Damping coeff. between sprung and unsprung mass
X_0	Road excitation input
X	Sprung mass bounce
φ	Sprung mass roll
θ	Sprung mass pitch
X_i	Unsprung mass bounce
i	Subscript referring 1, 2, 3 & 4

1. Introduction

Road vehicles experience vibrations while moving, mainly due to road surface irregularities, engine excitation forces, aerodynamic forces etc. Road induced vibrations can be isolated by well-designed suspensions systems. Automotive suspensions have been designed to satisfy conflicting requirements of better ride comfort, road handling and suspensions working space. Better ride comfort requires a soft suspension, whereas a stiffer suspension is required for a better control of both body and wheel as well as to provide adequate working space between the chassis and the car body. Due to these conflicting demands, the suspension designer has to balance the requirements of the ride comfort, road handling and suspension working space in different measures depending on the type of vehicle like a passenger car, truck, off road vehicle etc.

Automobiles were initially developed as self-propelled versions of horse-drawn vehicles. However, horse-drawn vehicles had been designed for relatively slow speeds and their suspension was not well suited for higher speeds as per internal combustion engine requirements. The first workablespring-suspension required advanced metallurgical knowledge and skill, and only became possible with the advent of industrialization. Obadiah Elliott registered the first patent for a spring-suspension vehicle; each wheel had two durable steel leaf springs on each side and the body of the carriage was fixed directly to the springs attached to the axles. Within a decade, most British horse carriages were equipped with springs; wooden springs in the case of light one-horse vehicles to avoid taxation, and steel springs in larger vehicles. These were often made of low-carbon steel and usually took the form of multiple layer leaf springs.

A semi-active suspension system is an unusual combination of seemingly simple dynamics and challenging features (nonlinear behaviour, time-varying parameters, asymmetrical control bounds, un-controllability at steady-state, etc.). These features make the design of semi-active control algorithms very challenging. This gives opportunity to use the control

strategy with an ease to modify significantly the dynamic behaviour of the vehicle. The history of semi-active suspensions is full of anecdotes about semi-active suspensions being rejected by vehicle manufacturers just because they "do not make any difference" or even "are worse than the (nice, old) traditional mechanical suspensions. As in many other electronically controlled systems, the actuator is not smart itself. Physical model for investigation of vertical dynamics of the suspension systems are most commonly built on the quarter car model. Quarter car is a 2 DoF system to study the characteristics of vehicle suspension system like ride comfort and road holding by considering the vertical vibration of sprung mass and unsprung mass [1-3]. Unsprung mass is linked to the ground with a tire modelled by stiffness and to the sprung mass with a suspension made up of a linear shock absorber and a linear spring [4-6].

Half car model having 4 DoF is used to study the pitching/rolling characteristics of the vehicle suspension system along with the bounce of sprung and unsprung mass [7-9]. Accuracy of evaluation can also be improved compared to quarter car model. Full car model having 7 DoF is made up with sprung mass in vertical translation and its rotation about two horizontal axes and the four unsprung masses bounce [10-14]. A full car model gives accurate results when investigated for vibration response. Pitch, roll and bounce modes of the sprung mass may also be analysed simultaneously with the help of full-car model, however different control strategies may be compared with quarter car model easily [15]. Semi-active suspension system consists of spring and damper with variable damping coefficient achieved by using MR damper, ER damper, variable orifice dampers and tuned liquid dampers. Semi-active suspension system's main task is to provide a high level of ride comfort by isolating the chassis mass from road disturbances and to improve road holding by preventing the wheel from losing road contact [16-20]. A semi-active suspension system performs better in improving the ride comfort and road handling keeping the complexity and cost at minimum [9, 11]. The semi active suspension system incorporates a damper that can modulate its damping coefficient. Semi-active systems are classified as systems where the characteristics can be changed rapidly (typically in less than 100 milliseconds).

The objective of this work is to develop a full car model of 7 DoF with semi active suspension system. The damped natural frequencies and the corresponding mode shapes for various damping values are found using analytical and numerical analysis. A comparison is drawn between the natural frequencies obtained for various damping values as well as between the natural frequencies obtained in ANSYS and MATLAB.

2. Mathematical modelling

Mathematical model of a 7 DoF passenger car is formulated using Newton's method. The kinematic effects due to suspension geometry are ignored i.e. the suspensions only provide vertical forces to the chassis. The model is formulated using linear conditions. Non-linear terms are ignored. The vehicle chassis plane is considered parallel to the road while usually cars are bent over to improve air penetration and reduce aero-dynamical resistance. For semi-active suspension system the hysteresis behaviour of the damper is neglected. In the analysis, sprung mass (M) is considered as rigid body. A schematic of the mathematical model is shown in Fig. 1. Three DoF are assigned to sprung mass i.e. bounce, pitch, and roll. Single DoF i.e. bounce is assigned to each of the unsprung mass. The bounce for sprung mass (M), front right unsprung mass (M_2), front left unsprung mass (M_1), rear right unsprung mass (M_3) and rear left unsprung mass (M_4) are computed using Eqns. (1) to (5) respectively. The sprung mass pitch (θ) and roll (φ) are computed using Eqns. (6) and (7) respectively.

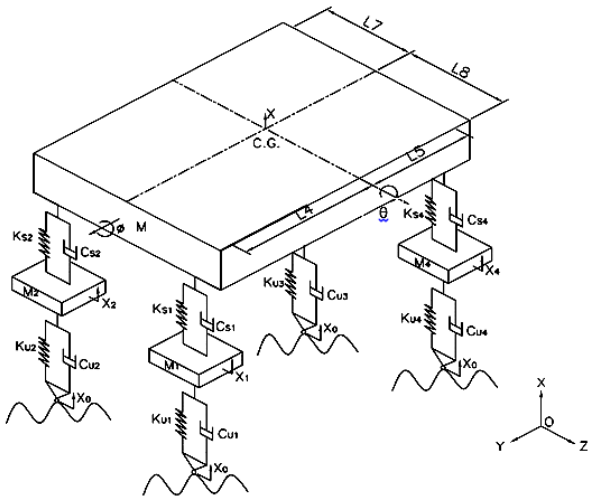

Fig. 1: A vertical full-car model with 7-DOF

$$M\ddot{X}+(K_{S1}+K_{S2}+K_{S3}+K_{S4})X-K_{S1}X_1-K_{S2}X_2-K_{S3}X_3-K_{S4}X_4+((K_{S1}+K_{S2})L_4-(K_{S3}+K_{S4})L_5)\theta+((K_{S1}+K_{S4})L_8-(K_{S2}+K_{S3})L_7)\varphi$$
$$+(C_{S1}+C_{S2}+C_{S3}+C_{S4})\dot{X}-C_{S1}\dot{X}_1-C_{S2}\dot{X}_2-C_{S3}\dot{X}_3-C_{S4}\dot{X}_4+((C_{S1}+C_{S2})L_4-(C_{S3}+C_{S4})L_5)\dot{\theta})+((C_{S1}+C_{S4})L_8-(C_{S2}+C_{S3})L_7)\dot{\varphi}=0 \quad (1)$$

$$M_2\ddot{X}_2-K_{S2}X+(K_{S2}+K_{U2})X_2-K_{S2}L_4\theta+K_{S2}L_7\varphi-K_{U1}X_0-C_{S2}\dot{X}+(C_{S2}+C_{U2})\dot{X}_2-C_{S2}L_4\dot{\theta}+C_{S2}L_7\dot{\varphi}-C_{U1}\dot{X}_0=0 \quad (2)$$

$$M_1\ddot{X}_1-K_{S1}X+(K_{S1}+K_{U1})X_1-K_{S1}L_4\theta-K_{S1}L_8\varphi-K_{U1}X_0-C_{S1}\dot{X}+(C_{S1}+C_{U1})\dot{X}_1-C_{S1}L_4\dot{\theta}-C_{S1}L_8\dot{\varphi}-C_{U1}\dot{X}_0=0 \quad (3)$$

$$M_3\ddot{X}_3-K_{S3}X+(K_{S3}+K_{U3})X_3+K_{S3}L_4\theta+K_{S3}L_7\varphi-K_{U3}X_0-C_{S3}\dot{X}+(C_{S3}+C_{U3})\dot{X}_3+C_{S3}L_4\dot{\theta}+C_{S3}L_7\dot{\varphi}-C_{U3}\dot{X}_0=0 \quad (4)$$

$$M_4\ddot{X}_4-K_{S4}X+(K_{S4}+K_{U4})X_4+K_{S4}L_5\theta-K_{S4}L_8\varphi-K_{U4}X_0-C_{S4}\dot{X}+(C_{S4}+C_{U4})\dot{X}_4+C_{S4}L_5\dot{\theta}-C_{S4}L_8\dot{\varphi}-C_{U4}\dot{X}_0=0 \quad (5)$$

$$I\ddot{\theta}+((K_{S1}+K_{S2})L_4-(K_{S3}+K_{S4})L_5)X-K_{S1}L_4X_1-K_{S2}L_4X_2+K_{S3}L_5X_3+K_{S4}L_5X_4+((K_{S1}+K_{S2})L_4^2+(K_{S3}+K_{S4})L_5^2)\theta$$
$$+(K_{S1}L_8L_4-K_{S2}L_7L_4+K_{S3}L_7L_5-K_{S4}L_8X_5)\varphi+((C_{S1}+C_{S2})L_4-(C_{S3}+C_{S4})L_5)\dot{X}-C_{S1}L_4\dot{X}_1-C_{S2}L_4\dot{X}_2+C_{S3}L_5\dot{X}_3+C_{S4}L_5\dot{X}_4 \quad (6)$$
$$+((C_{S1}+C_{S2})L_4^2+(C_{S3}+C_{S4})L_5^2)\dot{\theta}+(C_{S1}L_8L_4-C_{S2}L_7L_4+C_{S3}L_7L_5-C_{S4}L_8L_5)\dot{\varphi}=0$$

$$I\ddot{\varphi}+((K_{S1}+K_{S4})L_8-(K_{S2}+K_{S3})L_7)X-K_{S1}L_8X_1+K_{S2}L_7X_2+K_{S3}L_7X_3-K_{S4}L_8X_4+(K_{S1}L_8X_4-K_{S2}L_7X_4+K_{S3}L_7X_5 -K_{S4}L_8X_5)\theta+((K_{S1}+K_{S8})L_8^2+(K_{S2}+K_{S3})L_7^2)\varphi+((C_{S1}+C_{S4})L_8-(C_{S2}+C_{S3})L_7)\dot{X}-C_{S1}L_8\dot{X}_1+C_{S2}L_7\dot{X}_2+C_{S3}L_7\dot{X}_3 -C_{S4}L_8\dot{X}_4+(C_{S1}L_8L_4-C_{S2}L_7L_4+C_{S3}L_7L_5-C_{S4}L_8L_5)\dot{\theta}+((C_{S1}+C_{S8})L_8^2+(C_{S2}+C_{S3})L_7^2)\dot{\varphi}=0 \quad (7)$$

Table 1: Light weight passenger car vehicle parameters

Parameters (Symbols)	Value
Sprung mass (M)	656 kg
Mass mom. of inertia for vehicle body (I_y ,I_z)	1000, 500 kg-m^2
C.G distance from front axle (L_4)	0.8 m
C.G distance from rear axle (L_5)	1.29 m
Wheel track(L_7 and L_8)	0.87 m
Spring stiff. of front axle susp. (K_{S1} and K_{S2})	15000 N/m
Spring stiff. of rear axle susp. (K_{S3} and K_{S4})	8650 N/m
Damp. coeff. of front axle susp. (C_{S1} & C_{S2})	1189 N-s/m
Damp. coeff. of rear axle susp. (C_{S3} and C_{S4})	802 N-s/m
Stiffness of front tires (K_{U1}, K_{U2})	150000 N/m
Stiffness of rear tires (K_{U3}, K_{U4})	150000 N/m
Damp. coeff. of front tires (C_{U1} and C_{U2})	1500 N-s/m
Damp. coeff. of rear tires (C_{U3} and C_{U4})	1500 N-s/m
Mass of front axle (M_1 and M_2)	41 kg
Mass of rear axle (M_3 and M_4)	46 kg

3. Finite element (FE) modelling

FE modeling of full car is done in ANSYS APDL. Sprung mass is assumed as lumped mass in modeling, set-1 element is taken as sprung mass and it is connected by MPC-184 elements to form a frame as shown in Fig. 2. Wheels are also modelled as lumped masses by using set-2 for front wheels and set-3 for rear wheels. Wheels stiffness and damping are also modelled using set-6 for both front and rear wheels. Finally, wheels and frame are connected by using set-4 and set-5 on front and rear wheels respectively. Finally, full car model is modelled in ANSYS by following the above steps.

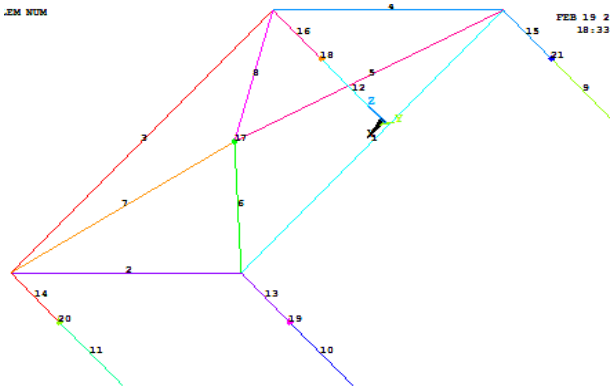

Fig. 2: Full-car model developed in ANSYS.

Table. 2: Real constants values for full-car model

Set #	Element type	Value
Set-1	MASS-21	M_1 = 656 kg, I_X= 500 kg-m^2, I_y = 1094 kg-m^2
Set-2	MASS-21	M_U = 41 kg
Set-3	MASS-21	M_U = 46 kg
Set-4	COMBIN-14	K_1,K_2 = 15000 N/m, C_1,C_2 = 1189 N-s/m
Set-5	COMBIN-14	K_3,K_4 = 15000 N/m, C_3,C_4 = 856 N-s/m
Set-6	COMBIN-14	K_U = 150000 N/m, C_U = 1500 N-s/m

4. Modal analysis

The first step in dynamic analysis of any system is to study its behaviour when it is just disturbed momentarily and then left to oscillate freely. The system vibrates at its natural frequencies. Natural frequencies and the corresponding mode shapes give important information about any dynamic system. When subjected to excitation, system vibrates at the frequency of excitation. The identified natural frequencies of the system help us to avoid resonant excitation frequencies by modifying the design. Both un-damped and damped modal analysis for the full car 7 DoF model is carried out to study the dynamic behaviour of the system at various damping coefficients.

4.1. Modal analysis of mathematical model

When damping is not considered, the equations of motion of the 7 DoF vehicle model can be written matrix form as,

$$[M]\{\ddot{x}\}+K\{x\}=0 \quad (8)$$

Where $[M]$ is the mass matrix of size 7×7, $[K]$ the stiffness matrix of size 7×7, and $\{x\}$ is the displacement vector of size 7×1. These equations can be rewritten in the form of a symmetric Eigen value problem by assuming a harmonic response as follows:

$$([K]-\omega^2[M])\{x)=0 \quad (9)$$

Where $\{x\}$ is the displacement amplitude vector of size 7×1. Solving the above eigenvalue problem, the un-damped natural frequencies and corresponding mode shapes are obtained.

When damping is considered, the equations of motion of the 7 DoF vehicle model can be written as,

$$[M]\{\ddot{x}\}+C\{\dot{x}\}+K\{x)=0 \quad (10)$$

Where $[C]$ is the damping matrix of size 7×7. These equations can be rewritten in the form of a symmetric eigenvalue problem by assuming a complex harmonic response as follows:

$$([K]-\omega^2[M]+i[C]\omega)\{X\}=0 \quad (11)$$

Where $\{x\}$ is the displacement amplitude vector of size 7×1. Solving the above eigenvalue problem, the damped natural frequencies and the corresponding mode shapes for different damping coefficients of the full car model are found.

Eigen analysis is carried out for the 7 DoF full car model to study the modal parameters like natural frequencies and corresponding mode shapes for different modes of vibration like pitch, roll and bounce for sprung mass and bounce for four unsprung masses. In Fig. 3 various modes of vibration for full car model may be observed. At natural frequency 10.03 Hz it is observed that bounce mode corresponding to unsprung masses 1, 2 are in phase with each other and vibrating with amplitude of 0.75 mm. At natural frequency 1.24 Hz bounce of sprung mass is occurring with an amplitude of

1 mm coupled with slight amplitude for unsprung masses bounce vibration due coupling of geometry. At frequency 1.02 Hz corresponding to roll mode of vibration is occurring with amplitude of 1 mm along with slight bounce for unsprung masses. At frequency 9.64 Hz amplitude of 0.6 mm has occurs for bounce mode unsprung mass 3, 4 and there are in phase with each other. At frequency 10.03 Hz masses 1, 2 are out phase and vibrating with amplitude of bounce is 0.6 mm. At natural frequency 9.63 Hz masses 3, 4 are vibrating in out-phase with amplitude 0.6 mm. Finally at natural frequency 1.14 Hz pitch mode of vibration is observed with amplitude of 1 mm along with the unsprung mass bounce due to coupling of system pitch should accompany by bounce variation in unsprung mass.

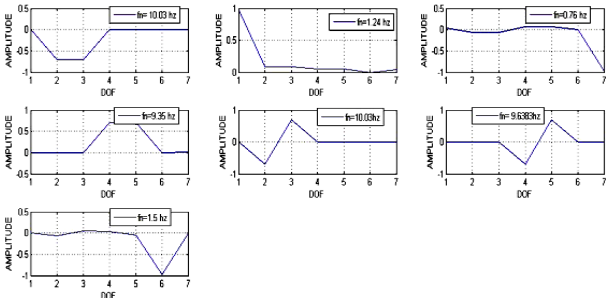

Fig. 3: Un-damped mode shapes of 7 DoF full-car model

Damping modal analysis of the 7 DoF full car model as shown in Table 1 is carried out by increasing the damping coefficient with a step size of 500 N-s/m upto 2000 N-s/m. In Fig. 4, modal analysis is carried out for damping coefficient equal to 500 N-s/m, and modal parameters are observed. Natural frequencies are slightly shifted by increasing damping coefficients to 500 N-s/m, the bounce mode natural frequency of for sprung-mass is increased from 1.24 Hz to 1.25 Hz. Natural frequency of unsprung mass 2 is decreased to 10.02 Hz from 10.03 Hz. Natural frequency of unsprung mass 3 is decreased from 9.38 Hz to 9.28 Hz. Similarly natural frequency of unsprung mass 4 is decreased from 9.34 Hz to 9.33 Hz. At natural frequency 1.25 Hz there is a slight decrease in amplitude of sprung mass bounce by 0.01 mm when compared to un-damped mode of vibration (Fig. 4). Similarly, there is slight decrease in amplitudes for four unsprung masses bounce and roll. However, there is no decrease in amplitude for pitch mode of vibration at natural frequency 1.5 Hz. The decrease in amplitude of sprung mass bounce is compensated in rolling due to normal vehicle coupling. The amplitude of vibration of the roll mode for sprung mass remained same that is 1 mm at natural frequency 0.77 Hz. At frequencies 10.02 Hz and 9.28 Hz unsprung masses 1, 2 and unsprung masses 3, 4 are in phase respectively and at frequencies 10.02 Hz and 9.33 Hz unsprung masses 1, 2 and unsprung masses 3, 4 are out of phase respectively.

The mode shapes of 7-DoF car model with the damping coefficient of 1000 N-s/m are shown in Fig. 5. Natural frequency of the bounce of unsprung mass 1 occurred at 10.00 Hz with amplitude of 0.6 mm (Fig. 5), unsprung mass 3 bounce occurred at 9.32 Hz with an amplitude 0.7 mm , roll mode of sprung mass occurred at 0.77 Hz with an amplitude 0.9 mm, bounce of sprung mass occurred at 1.26 Hz with an amplitude of 0.9 mm, bounce of unsprung mass occurred at 9.89 Hz and amplitude of 0.6 mm, bounce of unsprung mass 4 occurred at 9.09 Hz with an amplitude of 0.6 mm and pitch mode of vibration for sprung mass occurred at 1.51 Hz with an amplitude of 1 mm.

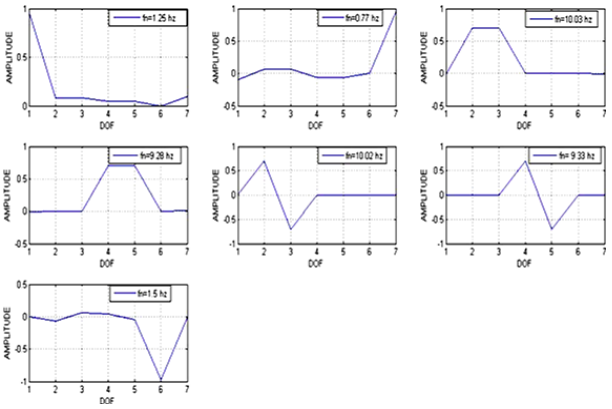

Fig. 4: Mode shapes of 7 DoF full-car model at C =500N-s/m

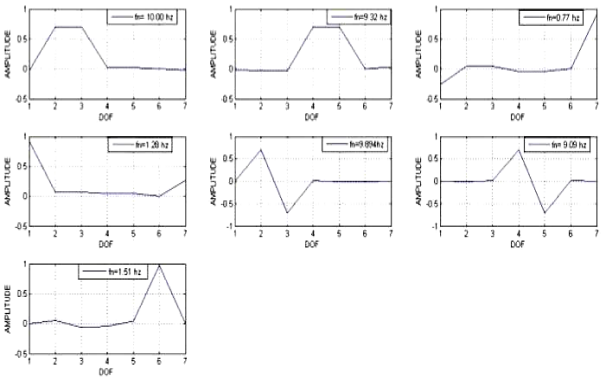

Fig. 5: Mode shapes of 7 DoF full-car model at C =1000N-s/m

Modal analysis is carried out for damping coefficient of C=1500 N-s/m and 7 modes of vibration of 7 DoF are shown in Fig. 6. It can also be observed that the bounce of unsprung mass 1 occurred at natural frequency at 9.96 Hz with an amplitude of 0.7 mm bounce of unsprung mass 3 is observed at 8.618 Hz and amplitude -0.7 mm, bounce of sprung mass occurred at 1.32 Hz and amplitude of 0.9mm, roll of sprung mass occurred at 0.77 Hz and amplitude of 0.9 Hz, bounce of unsprung mass2 occurred at 9.28 Hz and amplitude 0.6 mm, bounce of unsprung mass 4 occurred at 9.28 Hz and amplitude 0.6 mm, pitch of sprung mass occurred at 1.59 Hz and amplitude of 1mm.

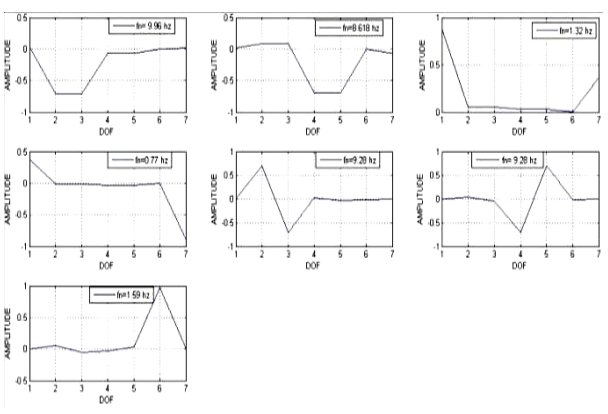

Fig. 6: Mode shapes of 7 DoF full-car model at C =1500 N-s/m

Modal analysis is carried out for damping coefficient C=2000 N-s/m and is as shown in Fig. 7. It is observed that modal shapes for bounce, pitch, roll of sprung mass occurred at 1.37 Hz, 1.59 Hz and 0.78 Hz with an amplitudes of 0.9 mm, 1 mm, and -0.6 mm respectively and bounce of unsprung masses 1, 2, 3 and 4 occurred at 9.88 Hz, 9.29 Hz, 9.24 Hz and 7.45 Hz with amplitudes 0.6 mm, 0.6 mm, -0.66 mm and 0.66 mm respectively. Natural frequencies and mode shape amplitudes thus obtained for various damping coefficients are shown in Table 3.

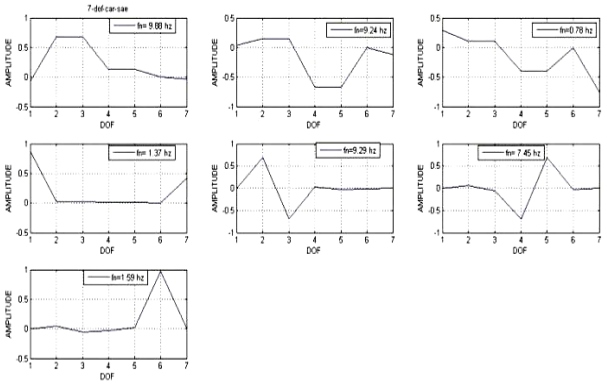

Fig. 7: Mode shapes of 7 DOF full-car model at C =2000 N-s/m

Table 3: Natural frequencies of the 7 DoF full car model for various damping coefficients in MATLAB

Modes	Frequency in Hz for various damping coeff. C [N s/m]				
	0	500	1000	1500	2000
Sprung mass roll	0.76	0.77	0.77	0.77	0.78
Sprung mass bounce	1.24	1.25	1.28	0.80	1.37
Sprung mass pitch	1.50	1.50	1.51	1.59	1.59
Unsprung mass 1 bounce	10.03	10.03	9.89	9.67	9.29
Unsprung mass 2 bounce	10.03	10.02	10.00	9.96	9.88
Unsprung mass 3 bounce	9.35	9.28	9.09	8.61	7.45
Unsprung mass 4 bounce	9.34	9.33	9.32	9.28	9.24

4.2. Modal analysis of FE model

Block Lanczos method is adopted for the un-damped modal analysis of the full car model based on the above description of the method. QR-Damped method is adopted for study of damped modal parameters of the 7 DoF full car model in ANSYS as shown in Fig. 2. This method is used to find out the damped natural frequencies and corresponding mode shapes for different values of damping coefficients. Since, the system is having 7 DoF therefore full car model will have 7 modes of vibration namely bounce, pitch and roll for sprung mass and bounces for 4 unsprung masses. Modal analysis is performed for 7 DoF full car model for the study of the modal parameters both for un-damped system and damped system for various damping coefficients ranging from 500-2000 N-s/m. From un-damped modal analysis of the full car, the mode shapes obtained are shown in Fig. 8. Mode shapes for bounce, pitch, roll of sprung mass occurred at 1.37 Hz, 1.59 Hz and 0.78 Hz with amplitudes of 0.9 mm, 1mm and -0.6 mm respectively. Bounce mode of unsprung masses 1, 2, 3, and 4 occurred at 9.88 Hz, 9.29 Hz, 9.24 Hz and 7.45 Hz with amplitudes 0.6 mm, 0.6 mm, -0.66 mm and 0.66 mm respectively.

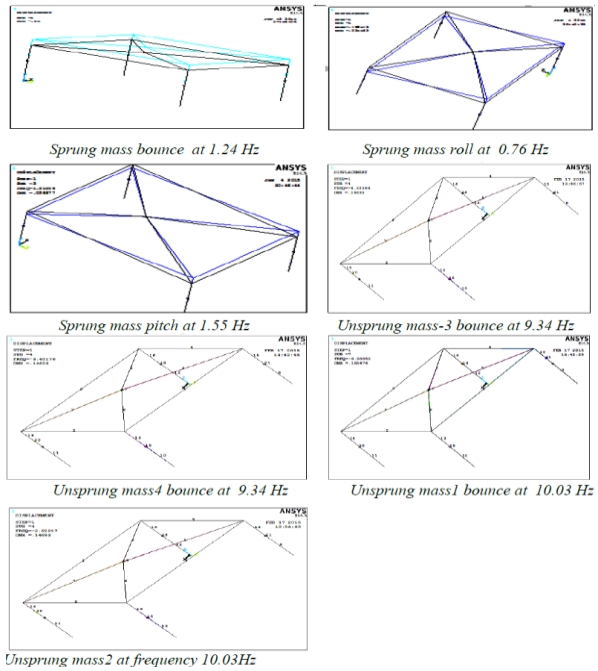

Fig. 8: Un-damped mode shapes of 7 DoF full-car model

The mode shapes for C=500 N-s/m are shown in Fig. 9. Mode shapes for bounce, pitch and roll of sprung mass occurred at 1.18 Hz, 1.57 Hz and 0.74 Hz with amplitudes of 0.9 mm, 1 mm and -0.6 mm respectively. The bounce mode of unsprung masses 1, 2, 3 and 4 occurred at 9.81 Hz, 9.81 Hz, 9.16 Hz and 9.16 Hz with amplitudes 0.15 mm, 0.15 mm, -0.15 mm and 0.15 mm respectively. With increase in damping, the mode shape corresponding to bounce is associated with rolling of the sprung mass due to coupling the system. The mode shapes for C = 1000 N-s/m are shown in Fig. 10. Mode shapes for bounce, pitch, roll of sprung mass occurred at 1.17 Hz, 1.47 Hz and 0.73 Hz with amplitudes of 0.03 mm, 0.05 mm and 0.06 mm respectively. Bounce modes of unsprung masses 1, 2, 3 and 4 occurred at 8.62 Hz, 8.62 Hz, 8.09 Hz and 8.17 Hz with amplitudes of 0.6 mm, 0.6 mm, -0.66 mm and 0.66 mm respectively.

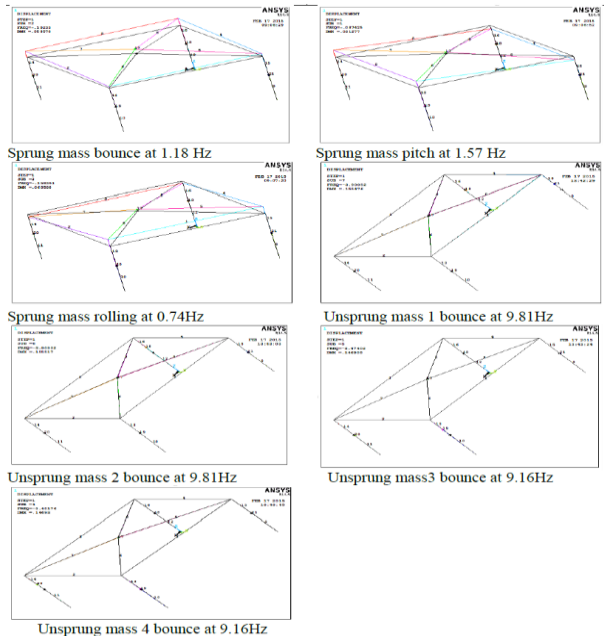

Fig. 9: Mode shapes of 7 DoF full-car model at d C =500 N-s/m

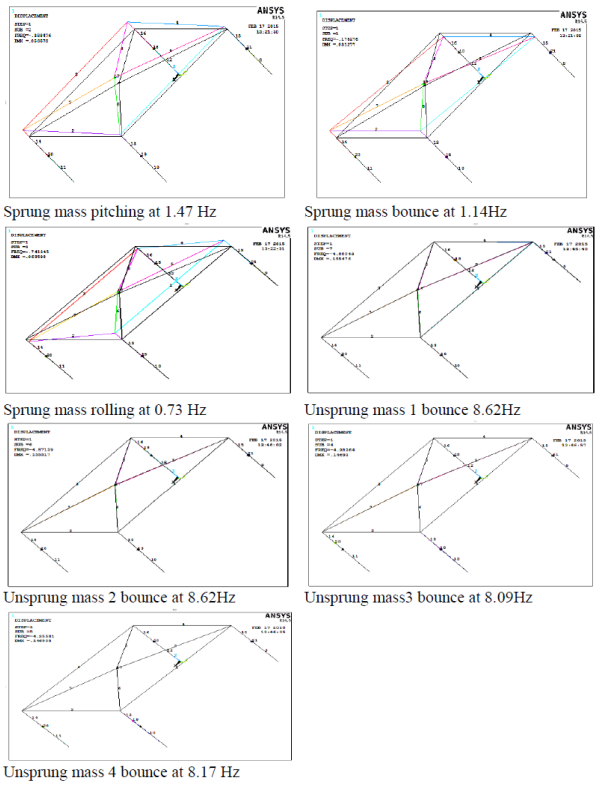

Fig. 10: Mode shapes of 7 DoF full-car at C = 1000 N-s/m

Mode shapes at C = 1500 N-s/m are shown in Fig. 11. Mode shapes for bounce, pitch and roll of sprung mass occurred at 1.06 Hz, 1.23 Hz and 0.72 Hz with amplitudes of 0.05 mm 0.06 and -0.03 mm respectively. Bounce modes of unsprung masses 1, 2, 3, 4 occurred at 7.9 Hz, 7.86 Hz, 7.1 Hz, and 7.4 Hz with amplitudes of 0.15 mm, 0.15 mm, -0.14 mm and 0.14 mm respectively. With increase in damping rolling vibrations are reduced due to increase in amplitude of car bounce.

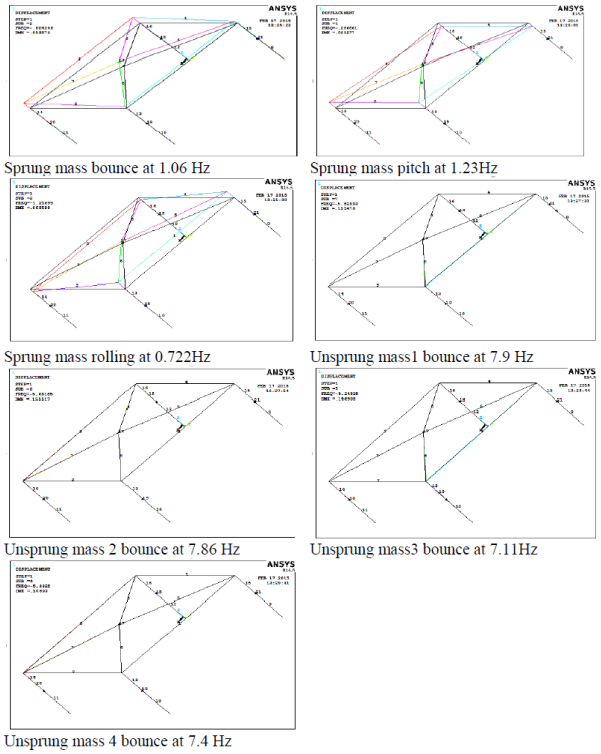

Fig. 11: Mode shapes of 7 DoF full-car at C = 1500 N-s/m

Mode shapes are obtained along with their natural frequencies for C = 2000 N-s/m which are shown as in Fig. 12. Mode shapes for bounce, pitch, roll of sprung mass occurred at 0.9 Hz, 1.23 Hz and 0.707 Hz with amplitudes of 0.04 mm, 0.06 mm, and 0.03 mm respectively. Bounce modes of unsprung masses 1, 2, 3, and 4 occurred at 6.73 Hz, 6.73 Hz, 6.4 Hz and 6.4 Hz with amplitudes of 0.14 mm, 0.14 mm, 0.13 mm and 0.13 mm respectively. With increase in damping coefficient pitching is associated with increase in amplitude of bounce for unsprung mass. A summary of the natural frequencies obtained in ANSYS are shown in Table 4. A comparison is drawn between the un-damped natural frequencies of the 7 DoF full car models that are obtained in MATLAB and ANSYS is given in Table 5.

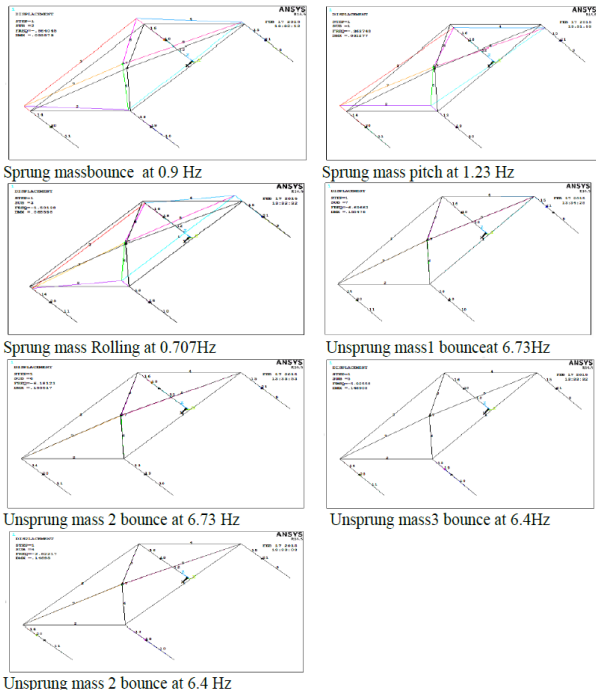

Fig. 12: Mode shapes of 7 DoF full-car at C = 2000 N-s/m

Table 4: Natural frequencies of the 7 DoF full car model for various damping coefficients in ANSYS

Modes	Frequency in Hz for various damping coeff. C [N s/m]				
	0	500	1000	1500	2000
Sprung mass roll	0.76	0.74	0.73	0.72	0.77
Sprung mass bounce	1.24	1.18	1.14	1.06	0.9
Sprung mass pitch	1.55	1.57	1.47	1.23	1.23
Unsprung mass 1 bounce	10.03	9.81	8.66	7.11	6.73
Unsprung mass 2 bounce	10.03	9.81	8.62	7.9	6.73
Unsprung mass 3 bounce	9.34	9.16	8.17	7.86	6.4
Unsprung mass 4 bounce	9.34	9.16	8.09	7.4	6.4

Table 5: Un-damped natural frequencies of 7 DoF full-car model

Mode of vibration	Modal analysis	
	MATLAB	ANSYS
Rolling	0.86	0.769
Car Bounce	1.24	1.2408
Pitching	1.45	1.5101
Wheel-1 bounce	10.03	10.037
Wheel-2 bounce	10.03	10.037
Wheel-3 bounce	9.35	9.3531
Wheel-4 bounce	9.35	9.3531

5. Conclusions

Un-damped and damped natural frequencies and the corresponding mode shapes for the 7 DoF full car model have been found from equations of motion and finite element method. The natural frequencies thus found by both the methods are in good agreement. The following are conclusions drawn from modal analysis of 7 DoF full car model. From un-damped modal analysis, mode shape of bounce of the sprung mass is associated with roll of the sprung mass due to the coupling of the system. Pitching of the sprung mass is independent of the roll and bounce of the sprung mass. From damped modal analysis, it is observed that natural frequencies of the full car model are shifting which will help us in avoiding the resonance of the system with road excitation during active/semi-active suspension systems.

REFERENCES:

[1] R.P. Kumar and S.R. Kulkarni. 2014. Comparative analysis of multiple controllers for semi-active suspension system, *Proc. of 2nd Int. Conf. on Emerging Research in Computing, Information, Communication and Applications*, Nitte Meenakhsi Institute of Tech., Bangalore, India.

[2] X. Dong, M. Yu and C. Liao. 2010. Comparative research on semi-active control strategies for magneto-rheological suspension, *Non Linear Dynamics*, 59(3), 433-453. https://doi.org/10.1007/s11071-009-9550-8.

[3] M.A. Eltantawie. 2012.Decentralized neuro-fuzzy control for half-car with semi-active suspension system, *Int. J. Automotive Technology*, 13(3), 423-431. https://doi.org/10.1007/s12239-012-0039-y.

[4] M.A. Karkoub and M. Zribi. 2006. Active/semi-active suspension control using magnetorheological actuators, *Int. J. Systems Science*, 37(1), 35-44. https://doi.org/10.1080/00207720500436344.

[5] S.M. Savaresi, E. Silani and S. Bittanti. 2005. An optimal control algorithm for comfort–oriented semi-active suspensions, *ASME Trans. J. Dyn. Sys. Meas. & Control*, 127(2), 218-229. https://doi.org/10.1115/1.1898241.

[6] S. Turkay and H. Akcay. 2010. Tire damping effect on h_2 optimal control of half-car active suspensions, *J. Vibration and Acoustics*, 132, 1-4. https://doi.org/10.1115/1.4000767.

[7] V. Goga and M. Klucik. 2012. Optimization of vehicle suspension parameters with use of evolutionary computation, *Procedia Engineering*, 48, 174-179. https://doi.org/10.1016/j.proeng.2012.09.502.

[8] X.M. Sun, Y. Chu, J. Fan and Q. Yang. 2012. Research of simulation on the effect of suspension damping on vehicle ride, *Energy Procedia*, 17, 145-151. https://doi.org/10.1016/j.egypro.2012.02.075.

[9] L.H. Zong, X.L. Gong, C.Y. Guo and S.H. Xuan. 2012. Inverse neuro-fuzzy MR damper model and its application in vibration control of vehicle suspension system, *Int. J. Vehicle Mech. and Mobility, Vehicle Sys. Dynamics*, 50(7), 1025-1041. https://doi.org/10.1080/00423114.2011.645489.

[10] L. Dugard, O. Sename, S. Aubouet and B.Talon. 2012. Full vertical car observer design methodology for suspension control applications, *Control Engineering practice*, 20, 832-845. https://doi.org/10.1016/j.conengprac.2012.04.008.

[11] A. Unger, F. Schimmack, B. Lohmann and R. Schwarz. 2013. Application of LQ-based semi-active suspension control in a vehicle, *Control Engineering Practice*, 21, 1841-1850. https://doi.org/10.1016/j.conengprac.2013.06.006.

[12] N.M. Ghazaly and A.O. Moaaz. 2014. The future development and analysis of vehicle active suspension system, *IOSR J. Mechanical and Civil Engineering*, 11, 2014, 16-25.

[13] H.J. Kim, H.S. Yang and Y.P. Park. 2002. Improving the vehicle Performance with active suspension using road-sensing algorithm, *Computers and Structures*, 80, 1569-1577. https://doi.org/10.1016/S0045-7949(02)00110-4.

[14] A.J. Qazi, A. Khan, M.T. Khan and S. Noor. 2013. A parametric study on performance of semi-active suspension system with variable damping coefficient limit, *AASRI Procedia*, 4, 154-159. https://doi.org/10.1016/j.aasri.2013.10.024.

[15] Y. Liu, T.P. Waters and M.J. Brennan. 2003. A comparison of semi-active damping control strategies for vibration isolation of harmonic disturbances, *J. Sound & Vibration*, 280(1-2), 21-39. http://dx.doi.org/10.1016/j.jsv.2003.11.048

[16] B. Assadsangabi and M. Eghtesad. 2009. Hybrid sliding mode of control of semi-active suspension systems, *Smart Materials and Structures*, 18, 250-270. https://doi.org/10.1088/0964-1726/18/12/125027.

[17] T.R.M. Rao, G.V. Rao, K.S. Rao and A. Purushottam. 2010. Analysis of passive and semi-active controlled suspension systems for ride comfort in an Omnibus passing over a speed bump, *Int. J. Research of Reviews in Applied Sciences*, 5, 7-17.

[18] J. Wang and C. Song. 2013. Computer Simulation on Fuzzy control of semi-active suspension system based on the whole vehicle, *Int. J. Multimedia & Ubiquitous Engg.*, 8(6), 217-228. https://doi.org/10.14257/ijmue.2013.8.6.22.

[19] L. Balamurugan, J. Jancirani, and M.A. Eltanrawie. 2014. Generalized magnetorheological (MR) damper model and its application in semi-active control of vehicle suspension system, *Int. J. Automotive Technology*, 15(3), 419-427. https://doi.org/10.1007/s12239-014-0044-4.

[20] S. Dutta, S. Narahari and G. Chakraborty. 2013. Semi-active vibration isolation of a quarter car model under random road excitations using magnetorheological damper, *Proc. 1st Int. and 16th National Conf. on Machines and Mechanisms*, IIT Roorkee, India.